Tissue Sodium Concentration in Myocardial Infarction in Humans:

A Quantitative [23]Na MR Imaging Study[1]

Ronald Ouwerkerk, PhD, **Paul A. Bottomley, PhD**, **Meiyappan Solaiyappan, PhD**, **Amy E. Spooner, MD**, **Gordon F. Tomaselli, MD**, **Katherine C. Wu, MD**, and **Robert G. Weiss, MD**
From the Division of Magnetic Resonance Research, Department of Radiology (R.O., P.A.B., M.S.); and Cardiology Division, Department of Medicine (A.E.S., G.F.T., K.C.W., R.G.W.), Johns Hopkins University, School of Medicine, 601 N Caroline St, JHOC 4241, Baltimore, MD 21287-0845.

Abstract

Purpose—To prospectively determine whether the absolute tissue sodium concentration (TSC) increases in myocardial infarctions (MIs) in humans and whether TSC is related to infarct size, infarct age, ventricular dysfunction, and/or electrophysiologic inducibility of ventricular arrhythmias.

Materials and Methods—Delayed contrast material-enhanced 1.5-T hydrogen 1 (^{1}H) magnetic resonance (MR) imaging was used to measure the size and location of nonacute MIs in 20 patients (18 men, two women; mean age, 63 years ± 9 [standard deviation]; age range, 48-82 years) examined at least 90 days after MI. End-systolic and end-diastolic volumes, ejection fraction, and left ventricle (LV) mass were measured with cine MR imaging. The TSC in normal, infarcted, and adjacent myocardial tissue was measured on sodium 23 ([23]Na) MR images coregistered with delayed contrast-enhanced ^{1}H MR images. Programmed electric stimulation to induce monomorphic ventricular tachycardia (MVT) was used to assess arrhythmic potential, and myocardial TSC was compared between the inducible MVT and noninducible MVT patient groups.

Results—The mean TSC for MIs (59 μmol/g wet weight ± 10) was 30% higher than that for noninfarcted (remote) LV regions (45 μmol/g wet weight ± 5, $P < .001$) and that for healthy control subjects, and TSC did not correlate with infarct age or functional and morphologic indices. The mean TSC for tissue adjacent to the MI (50 μmol/g wet weight ± 6) was intermediate between that for the MI and that for remote regions. The elevated TSC measured in the MI at [23]Na MR imaging lacked sufficient contrast and spatial resolution for routine visualization of MI. Cardiac TSC did not enable differentiation between patients in whom MVT was inducible and those in whom it was not.

Conclusion—Absolute TSC is measurable with [23]Na MR imaging and is significantly elevated in human MI; however, TSC increase is not related to infarct age, infarct size, or global ventricular function. In regions adjacent to the MI, TSC is slightly increased but not to levels in the MI.

Tissue sodium levels are altered by cellular integrity and energy status in living mammalian cells. The resting potential of excitable tissues is the result of concentration gradients in sodium (Na^{+}), potassium (K^{+}), and chloride ions. Therefore, the ability to maintain a high extracellular sodium concentration and a low intracellular sodium concentration, at the cost of adenosine

triphosphate, by actively exchanging sodium and potassium ions through the Na^+/K^+ adenosine triphosphatase channel is crucial to the functioning of myocytes (1) and other excitable cells. If the adenosine triphosphate supply is insufficient because the cellular energy metabolism is impaired or challenged (2,3), or if the cell membrane integrity is compromised (4), low intracellular sodium concentration levels can increase sharply.

Advances in Knowledge

- Myocardial tissue sodium concentration (TSC) is significantly ($P < .001$) elevated in myocardial infarction (MI) in humans, regardless of MR relaxation effects.

- The myocardial TSC remote from an MI is normal.

- For infarcts older than 90 days, we found no clear correlation between infarct age and TSC ($r^2 = 0.008$).

- For infarcts older than 90 days, we found no clear correlation between TSC measured at rest and inducibility of arrhythmia: The MI TSC in the patients in whom monomorphic ventricular tachycardia (MVT) was inducible was not significantly different ($P > .05$) from that in the patients in whom MVT was not inducible.

Sodium 23 (^{23}Na) magnetic resonance (MR) imaging can be used to detect increased tissue sodium signal intensity in healthy subjects after exhaustive exercise (5-7) and to detect larger increases in acute myocardial infarction (MI) in dogs (8) and isolated rat (9) hearts. These changes may be attributable to loss of cellular integrity, inhibition of the Na^+/K^+ adenosine triphosphatase function as a result of energy depletion, changes in the ratio of intracellular-to-extracellular volume (8,9), and possibly molecular-level changes in the sodium ion environment. Increased myocardial signal intensity at ^{23}Na MR imaging has been observed in patients with chronic MI (10), with the elevations gradually declining with infarct age (11). Because of the methods used to acquire those data, there remains the question of whether the observed signal intensity changes after MI are due to physiologic changes in the actual tissue sodium concentration (TSC) or to molecular-level changes that affect the spin-lattice (T1) and spin-spin (T2) MR relaxation properties of sodium.

Although there currently is no safe, reliable way to unambiguously separate the signals of extra- and intracellular sodium in the heart of humans, the potential role of relaxation changes can be effectively eliminated by using MR imaging methods that minimize the influence of T1 and T2 relaxation times on the observed ^{23}Na signal. Thus, with the use of a fully relaxed ultrashort-echo-time twisted projection ^{23}Na MR imaging pulse sequence, the absolute TSC has been noninvasively quantified in human skeletal muscle (5) and in the healthy heart (12). The same methods used in an acute canine MI model have revealed elevated TSC, which was validated with atomic absorption spectroscopy (8). To date, however, these methods have not been applied to human MI.

Implication for Patient Care

- Ultrashort-echo-time ^{23}Na MR imaging at 1.5 T can be used to noninvasively quantify myocardial TSC in patients.

We hypothesized that the reported ^{23}Na MR imaging signal intensity changes seen after MI are due primarily to physiologic elevations in cardiac TSC and not to changes in ^{23}Na MR T1 and T2 relaxation times. The infarcted region itself is irreversibly injured and may act as a barrier to the propagation of the cardiac excitation wave. Altered sodium concentrations in the

surrounding tissue (13) could also affect excitation and predispose the heart to life-threatening arrhythmias (1,14). We therefore also hypothesized that the TSC in MIs, regions adjacent to the MI, and/or remote left ventricular (LV) regions may correlate with susceptibility to arrhythmia, as assessed with inducibility testing at electrophysiologic examination. Thus, the purpose of our study was to prospectively determine whether the absolute TSC increases in human MIs and whether TSC is related to infarct size, infarct age, ventricular dysfunction, and/or electrophysiologic inducibility of ventricular arrhythmias.

Materials and Methods

Patient Group

Twenty patients (18 men, two women; mean age, 63 years ± 9 [standard deviation]; age range, 48-82 years) who had a history of prior MI and were consecutively recruited for ^{23}Na and hydrogen 1 (^{1}H) MR imaging and contrast material-enhanced functional ^{1}H MR imaging were examined 94-7915 days (mean, 2738 days ± 2553) after MI. The age of the MI in three patients was unknown. No clinically recognized events had occurred within the past 90 days. Our Health Insurance Portability and Accountability Act-compliant study was approved by the Johns Hopkins University Institutional Review Board, and all patients gave written informed consent. Patient inclusion criteria were history of prior MI, LV ejection fraction of 35% or lower, and referral for cardiac defibrillator implantation as a primary prevention. Patients with pacemakers, implanted cardiac defibrillators, or metallic implants were excluded. We previously used the twisted projection ^{23}Na MR imaging method described herein to measure the cardiac TSC in 10 healthy male volunteers (mean age, 39 years ± 8; age range, 24-49 years) with no history of cardiovascular disease (12), and these data were used in our current study for statistical comparisons with the data obtained in patients.

Examination 1: Contrast-enhanced and Functional MR Imaging

To determine the cardiac morphologic and functional parameters and the location and size of the MIs, we performed a separate ^{1}H MR examination that consisted of cine and delayed contrast-enhanced MR image acquisitions conducted with a 1.5-T MR unit (Signa CV/i; GE Healthcare Technologies, Waukesha, Wis) and a four-element cardiac phased-array receiver coil placed anteriorly and posteriorly over the chest. After scout images were acquired to locate the heart, 10-12 contiguous short-axis cine sections were prescribed to encompass the entire LV from the base to the apex. Cine images were then acquired with a steady-state free precession pulse sequence (3.8/1.6 [repetition time msec/echo time msec], 45° flip angle, 36-40-cm field of view, 8-mm section thickness, 256 × 160 matrix, temporal resolution of 40 msec) to measure the LV mass, end-systolic and end-diastolic volumes, and LV ejection fraction. Delayed contrast-enhanced images were acquired 15-30 minutes after an injection of 0.2 mmol of gadodiamide (Omniscan; GE Healthcare Technologies) per kilogram of body weight by applying an inversion-recovery fast gradient-echo pulse sequence to the same short-axis locations as those on the cine images and a cardiacgated 300-msec delay after the R wave (5.4/1.3/150-250 [repetition time msec/echo time msec/inversion time msec, adjusted to null normal myocardial signal], 20° flip angle, 36-40-cm field of view, 8-mm section thickness, 256 × 192 matrix, two signals acquired).

Examination 2: ^{23}Na MR Imaging

To quantify the TSC in infarcted and noninfarcted regions with ^{23}Na MR imaging and to coregister the ^{23}Na images with the contrast-enhanced ^{1}H images, a combined ^{1}H and ^{23}Na MR examination was performed not more than 48 hours after the delayed contrast-enhanced MR examination. First, to generate a black blood cardiac image, ^{1}H images were acquired while the subject was lying on the ^{23}Na MR imaging body coil with phantoms embedded in place; an axial cardiac-gated ^{1}H fast spin-echo sequence (repetition time, 1 · R-R; echo time,

17 msec) was used. Second, a fast gradient-echo sequence (cardiac-gated 45-msec delay after R wave, 8.9/2.0, 75° flip angle, 5.0- or 7.5-mm section, 2.5-mm intersection spacing, 256 × 192 matrix, 36-cm field of view) was applied by using a transmit-receive body coil. The fast spin-echo and fast gradientecho images were used to define the ventricular wall. Next, three-dimensional ^{23}Na MR imaging (echo time, 0.4 msec) was performed with a square 25 × 25-cm ^{23}Na surface coil at 16.9 MHz by using a 1240-projection twisted projection imaging sequence and a 0.4-msec tanh/tan amplitude- and frequency-modulated adiabatic pulse to obtain fully relaxed ^{23}Na images. The spatial resolution was 6 mm isotropic, with 0.2-mL voxels. In nine patients, the ^{23}Na MR examination could not be gated to the heart rate because of an unreliable pulse signal. In these patients, a repetition time of 100 msec was used with six acquired signals such that the imaging time was approximately 12.4 minutes. In all other patients, the images were cardiac gated with a 150-msec delay after the trigger and a repetition time of 85 msec for up to 70%-80% of the R-R interval and imaging times of approximately 15-20 minutes.

Finally, ^{23}Na images were obtained in a 150 mmol/L Na$^+$ concentration reference phantom by using the same acquisition parameters (100/0.4). The signals from three tubes containing 100 mmol/L sodium chloride in agarose gel that were embedded in the coil were used to correct for differences in coil loading between the patient and phantom examinations. These tubes also served as fiducial markers for coregistration of the ^{23}Na images with the ^{1}H images and concentration reference images.

Image Analysis and TSC Calculation

The delayed contrast-enhanced MR data were analyzed by using a custom software package (CINEtool; GE Healthcare Technologies). A simplified version of the full-width half-maximum method (15) was used to define the MI. First, the endocardial and epicardial borders were traced by hand (K.C.W., A.E.S., 10 and 2 years experience, respectively), and the maximal signal intensity in this region was determined. In each patient, highly enhancing regions on each short-axis section were measured with planimetry, and the sizes of these regions were expressed in grams of myocardial tissue (15). The raw data from the 1240 projections of the ^{23}Na images were resampled onto a 64 × 64 × 64 point grid before Fourier transformation to yield three-dimensional images (12).

The ^{1}H fast spin-echo and fast gradient-echo MR images were coregistered with the ^{23}Na images generated from the ^{23}Na examination by using custom software developed in Matlab (Mathworks, Natick, Mass). The separately acquired delayed contrast-enhanced MR images were first coregistered with the ^{1}H body-coil scout images acquired at ^{23}Na MR imaging by using a three-dimensional workstation and computer software system (Dextroscope; Volume Interactions, Singapore). The infarctions were outlined on the contrast-enhanced images (A.E.S., M.S., 8 years experience), their locations were matched on the ^{1}H fast spin-echo or fast gradient-echo body coil images (Fig 1), and these images were in turn aligned with the ^{23}Na images for quantitation of the TSC in the different regions. The matches were optimized for analysis of the area containing the MI. Coregistration of the ^{23}Na MR images with the ^{1}H MR images acquired from the same examination was based on position information in the image header, with slight adjustments for the MR frequency based on the fiducial markers present on both images. Coregistration of the contrast-enhanced and ^{1}H fast spin-echo images generated from the ^{23}Na MR examination was better when cardiac gating was performed.

The TSC was quantified in regions of interest (ROIs) in blood, adipose tissue, MI, and remote and adjacent myocardial tissue that were manually drawn (R.O., 15 years cardiac MR experience) on the registered ^{1}H images such that a 2-pixel margin was maintained between the myocardial ROIs and the blood pool to minimize contamination (Fig 2). The same methods used to place ROIs were applied (R.O.) to determine the TSC in myocardial, blood, and adipose

tissue in the healthy volunteers from the earlier study (12), who were included in the current study for comparison. Adjacent ROIs were defined as non-MI regions with areas of at least 4 cm^2 that extended not more than 3 cm from the edge of the MI. Because of registration difficulties and the irregular shape of the MI, these regions were measured in about half ($n = 11$) the patients. ROIs for each target tissue were selected on two or more sections, the number of which depended on the extent and position of the MI. All the ROI boundaries set on the ^{1}H MR images were copied to the coregistered ^{23}Na MR images.

TSC was determined from the ratio of the mean ROI signal to the mean signal measured in the same location on the separately recorded coregistered image of the concentration reference phantom. This signal intensity ratio was corrected for coil loading by using the signal intensities of coil phantoms previously validated and described in detail (12). The TSC values calculated for multiple ROIs in the same tissue type were averaged for each patient. The calculation of a TSC map from the cardiac image-to-reference sodium image ratio on a pixel-by-pixel basis is highly susceptible to noise induced by the division operation—particularly away from the coil—and thus does not result in a reliable image. Therefore, for display purposes only, ^{23}Na image signal intensity was adjusted for local variations in the sensitivity of the receiver coil by using a computer-generated radiofrequency magnetic induction field (B$_1$) estimate of the coil. The computed B$_1$ correction amplifies noise in low-signal-intensity areas, but it does not add noise to the image. For myocardial and adipose tissue, TSC values were expressed in micromoles per gram wet weight with the assumption of specific gravities of 1.05 g/mL for the myocardium (16) and 0.90 g/mL for adipose tissue (17). For blood, a specific gravity of 1.00 g/mL was assumed.

Electrophysiologic Evaluation

In 16 of the 20 patients, programmed ventricular stimulation through an implanted cardiac defibrillator had been performed at the time of defibrillator implantation (clinically indicated) in a separate electrophysiologic study (18,19). The stimulation protocol consisted of three extra stimuli applied for two drive cycle lengths and delivered from the right ventricular apex alone (via implanted cardiac defibrillator) or from the right ventricular apex and the outflow tract. The induction of sustained monomorphic ventricular tachycardia (MVT) that lasted for 30 seconds or longer or required cardioversion owing to hemodynamic compromise was used to determine the inducibility of ventricular arrhythmia (G.F.T., 18 years experience in cardiac electrophysiology).

Statistical Analyses

TSC values in the MI, remote LV wall, and adjacent LV wall were compared by using a Student *t* test. For multiple comparisons, we applied the Bonferroni-corrected *t* test (correction factor, κ= 3). Regional differences in cardiac TSC were also compared by using Wilcoxon ranked parametric tests. We used an unpaired *t* test to compare the TSC in remote LV regions with previously published TSC values that were measured in healthy volunteers by using the same ^{23}Na MR imaging technique (12). Pearson product moment correlations *(r)* were used to test for correlations between TSC and infarct size, LV mass, and infarct age. We used a two-tailed unpaired *t* test to test for differences in MI, adjacent LV, and remote LV TSC between the patients in whom MVT was inducible and those in whom it was not inducible. All *t* tests and Pearson product moment correlations were performed by using Excel, version 11.3.3 2004, software (Microsoft, Redmond, Wash). Differences indicated by *P* < .05 were considered to be significant, unless otherwise indicated owing to corrections for multiple comparisons.

Results

Image Coregistration

We compared the anatomic fast spin-echo ^{1}H MR images and coregistered [23]Na MR images by overlaying the signal intensity contours and colors (Fig 3). The identification of infarcted regions on the [23]Na images alone was not obvious. Superimposing these images over the dark blood ^{1}H MR images improved visualization of the MIs on the [23]Na images (Fig 3). The adjacent zones bordering the MIs were identified with delayed contrast-enhanced MR imaging for TSC quantification in 11 of the 20 patients.

TSC Values

The blood TSC in the patients was not significantly different from the blood TSC previously measured in healthy subjects (12) (Table). The pooled TSC for right ventricular and LV blood in the patients was 73 mmol/L $\pm$ 11 compared with a pooled TSC of 79 mmol/L $\pm$ 8 for the control subjects (12) ($P > .05$). For adipose tissue, the mean TSC was 16 μmol/g wet weight $\pm$ 5 in the patients versus 17 μmol/g wet weight $\pm$ 4 in the control subjects ($P > .05$) (Table).

The mean TSC for the noninvolved remote LV in the 20 patients was 45 μmol/g wet weight $\pm$ 5. The mean TSC for MI regions, 59 μmol/g wet weight $\pm$ 10, was significantly elevated—by about 30%—compared with that for the remote noninvolved regions ($P < .001$, two-tailed paired t test) (Fig 4). The mean TSC for the myocardial tissue adjacent to the MI was 50 μmol/g $\pm$ 6, which was intermediate between and similar to the mean TSC values for the MI and the remote LV regions; differences were nonsignificant after Bonferroni correction. In addition, the TSC in the infarcted myocardium was significantly higher than the cardiac TSC previously measured in healthy volunteers (12) ($P < .001$, two-tailed t test with assumption of unequal variance).

Infarct Age, Cardiac Function, and Arrhythmia Inducibility

At more than 90 days after infarction, MI TSC was not related to infarct age ($r = 0.09$) (Fig 5). Also, the TSC in the MI, adjacent tissue, and noninvolved LV showed no significant correlation with end-diastolic volume, ejection fraction, absolute infarct size, or LV mass (Fig 6). Finally, TSC values in the MI, adjacent tissue, and remote zones were similar between the patients in whom MVT was inducible and those in whom MVT was not inducible ($P > .05$) (Fig 7), and they did not enable the determination of arrhythmia inducibility on an individual basis.

Discussion

Although elevated signal intensity in human MI has previously been demonstrated at noninvasive [23]Na MR imaging (20,21), to our knowledge, our study is the first in which the absolute TSC was quantified in human MI. Quantifying the absolute TSC has practical value because it enables one to determine whether differences in TSC exist from one subject to another and to determine the magnitude of any such differences. Absolute TSC quantification enabled, for the first time, to our knowledge, a comparison of remote myocardial tissue in patients with MI with corresponding myocardial tissue in healthy subjects. The mean TSC of 45 μmol/g wet weight $\pm$ 5 for the remote LV regions in our study was not significantly different from the previously reported value of 43 μmol/g wet weight $\pm$ 4 for the LV regions in healthy volunteers (12). These values are somewhat higher than previously obtained invasive and noninvasive measurements in canine hearts—31 μmol/g $\pm$ 7 and 34 μmol/g $\pm$ 3, respectively (8)—but similar to the reference value of 53 μmol/g for the human heart (17).

Thus, our results demonstrate that the mean absolute myocardial TSC was elevated by about 30% in human MI, while the TSC values in noninvolved myocardial tissue, blood, and adipose

tissue in patients with MI were comparable to previously reported absolute TSC values in healthy subjects (12). These results support the view that previous observations of elevated [23]Na MR imaging signal intensity in chronic MI are attributable to TSC increases and eliminate the confounding effects of the MR imaging relaxation times, T1 and T2.

The image contrast achieved by using the described twisted projection [23]Na MR imaging technique differs from the contrast previously observed with gradient-echo MR imaging techniques and the much longer echo times in patients with MI (11,22). Healthy myocardial tissue has an observable twisted projection signal intensity, but it is nearly invisible on gradient-echo images (11). Because it is easier to measure and quantify a high-signal-intensity area against a dark background than against a middletone background (23), there may be some advantage to using techniques involving longer echo times now that we have shown that such signal intensity changes do reflect TSC changes—albeit at the expense of [23]Na MR imaging signal-to-noise ratio. Because the MI TSC is intermediate between that of whole blood and that of normal myocardial tissue, the wall thinning associated with MI further hinders the visual identification of MI on many [23]Na MR images. Without careful coregistration of our three-dimensional [23]Na images with the delayed contrast-enhanced ^{1}H images, it would have been difficult to unambiguously distinguish MI from the nearby blood pools. Because blood is a possible source of signal contamination with the current [23]Na MR imaging spatial resolution used, a margin was maintained between the myocardial and blood pool ROIs to minimize errors. Future improvements in signal-to-noise ratio and spatial resolution achieved by using higher magnetic field strengths may improve the visual identification of infarcted and adjacent areas at [23]Na MR imaging.

Changes in the sodium concentration gradient across the cell membrane may lead to changes in the electrophysiologic properties of the myocardium. This may happen in the MI owing to scar formation in adjacent tissue, where necrotic and viable fiber bundles can coexist, as well as in remote or viable tissues during metabolic stress as a result of increased workload or compromised oxygen or substrate delivery during ischemia (24,25). A sodium concentration increase—even a temporary one—in these regions can alter ion channel and transporter function and may render the heart more susceptible to arrhythmias. In fact, many re-entrant arrhythmias are thought to arise in the border zone between infarcted and viable myocardium (26). Because infarct border zones are often heterogeneous, it is possible that the modest elevation in TSC measured in adjacent zones in this study may have been due in part to partial volume effects, with a contribution from neighboring MI. In future studies, efforts to further improve the spatial resolution of [23]Na MR imaging beyond that achieved at 1.5 T in the current study may facilitate a better understanding of TSC in zones adjacent to MI.

To determine whether quantitative [23]Na MR imaging has value in the prediction of arrhythmic potential, we related—for the first time, to our knowledge—TSC to MVT inducibility determined at the time of cardiac defibrillator implantation. We found that TSC values at rest were similar between patients in whom MVT was inducible and those in whom it was not. It may be more useful in future work to relate TSC to implanted cardiac defibrillator firings or sudden cardiac death events since these are better markers for sudden cardiac death risk than is MVT inducibility. Also, because life-threatening arrhythmias are infrequent and may be triggered by physiologic or pathologic stressors in patients at risk, the TSC measured during stress may be more predictive of an arrhythmogenic ionic milieu that is likely to trigger a lifethreatening arrhythmia than the measurements performed at rest in the current study.

We found that the MI TSC did not vary with the age of infarction in patients examined at least 90 days after their MI. This finding is consistent with a prior report of a modest but significant decrease in relative [23]Na MR imaging signal intensity through day 14 after MI, with no further significant decreases during the ensuing year (11).

In terms of study limitations, the previously examined healthy volunteers (12) were significantly younger than the patients with MI reported herein; thus, we cannot exclude the possibility that age was a confounding factor. However, the TSC in remote regions in the patients with MI agreed well with those in the healthy subjects, and comparisons between remote region TSC and MI TSC in the same subjects are not confounded by age. The number of patients who had arrhythmia inducibility findings was relatively modest. Although we cannot exclude the possibility that a significant difference in TSC could be identified in future studies involving larger numbers of patients, the present data strongly suggest that any differences in TSC between patients in whom MVT is inducible and those in whom it is not, if they exist, will be small in magnitude and thus will not enable differentiation of individual patients.

In conclusion, myocardial TSC is measurable with ^{23}Na MR imaging and is significantly elevated in MI and adjacent regions in humans; however, the increase in MI TSC does not appear to be related to infarct age or size or to global ventricular function. The increase in TSC occurs in infarcted regions and to a lesser degree in adjacent regions. The blood and adipose tissue TSC measured in patients in the current study was consistent with prior values measured in healthy subjects. The results suggest that prior observations of elevated ^{23}Na MR imaging signal intensity in patients with chronic MI were due to TSC increases and were not simply a confounding effect of MR relaxation time changes and that TSC increases extend to adjacent viable myocardial regions. Although intracellular ^{23}Na is important for myocellular excitability, it does not appear that the TSC measured at rest is closely associated with increased risk of arrhythmia, as assessed according to inducibility of MVT. Finally, we note that, unlike earlier ^{23}Na MR imaging approaches used to measure relative changes in sodium levels, measurement of absolute TSC with the twisted projection ^{23}Na MR imaging method described herein is well suited for studies of the role of sodium in contractile dysfunction in global heart disease, including cardiomyopathies.

Acknowledgments

Abbreviations

LV, left ventricle; MI, myocardial infarction; MVT, monomorphic ventricular tachycardia; ROI, region of interest; TSC, tissue sodium concentration.

References

1. Zipes, DP. Genesis of cardiac arrhythmias: electrophysiological considerations. In: Braunwald, E., editor. Heart disease: a textbook of cardiovascular medicine. 4th ed.. Saunders; Philadelphia, Pa: 1992. p. 602-627.

2. Askenasy N, Vivi A, Tassini M, Navon G. Cardiac energetics, cell volumes, sodium fluxes, and membrane permeability: NMR studies of cold ischemia. Am J Physiol 1995;269(3 pt 2)

3. Askenasy N, Vivi A, Tassini M, Navon G. The relation between cellular sodium, pH and volumes and the activity of Na/H antiport during hypothermic ischemia: multinuclear NMR studies of rat hearts. J Mol Cell Cardiol 1996;28:589–601. [PubMed: 9011642]

4. Ouwerkerk R, van Echteld CJ, Staal GE, Rijksen G. Erythrocyte Na+/K+ ATPase activity measured with ^{23}Na NMR. Magn Reson Med 1989;12:164–171. [PubMed: 2559285]

5. Constantinides CD, Gillen JS, Boada FE, Pomper MG, Bottomley PA. Human skeletal muscle: sodium MR imaging and quantification—potential applications in exercise and disease. Radiology 2000;216:559–568. [PubMed: 10924586]

6. Bansal N, Szczepaniak L, Ternullo D, Fleckenstein JL, Malloy CR. Effect of exercise on [23]Na MRI and relaxation characteristics of the human calf muscle. J Magn Reson Imaging 2000;11:532–538. [PubMed: 10813863]

7. Ouwerkerk, R.; Lee, RF.; Bottomley, PA. Dynamic changes in sodium levels in human exercising muscle measured with [23]Na MRI; Proceedings of ISMRM seventh scientific meeting and exhibition; Philadelphia, Pa. 1999; May 22-28. p. 1530

8. Constantinides CD, Kraitchman DL, O'Brien KO, Boada FE, Gillen J, Bottomley PA. Noninvasive quantification of total sodium concentrations in acute reperfused myocardial infarction using [23]Na MRI. Magn Reson Med 2001;46:1144–1151. [PubMed: 11746581]

9. Jansen MA, Nederhoff MG, van Echteld CJ. Intracellular sodium MRI in chronic myocardial infarction. J Cardiovasc Magn Reson 2004;6(1):439.

10. Horn M, Weidensteiner C, Scheffer H, et al. Detection of myocardial viability based on measurement of sodium content: a Na-23-NMR study. Magn Reson Med 2001;45:756–764. [PubMed: 11323801]

11. Sandstede JJ, Hillenbrand H, Beer M, et al. Time course of [23]Na signal intensity after myocardial infarction in humans. Magn Reson Med 2004;52:545–551. [PubMed: 15334573]

12. Ouwerkerk R, Weiss RG, Bottomley PA. Measuring human cardiac tissue sodium concentrations using surface coils, adiabatic excitation, and twisted projection imaging with minimal T_2 losses. J Magn Reson Imaging 2005;21:546–555. [PubMed: 15834912]

13. Jennings RB, Sommers HM, Kaltenbach JP, West JJ. Electrolyte alterations in acute myocardial ischemic injury. Circ Res 1964;14:260–269. [PubMed: 14133953]

14. Alvarez JL, Aimond F, Lorente P, Vassort G. Late post-myocardial infarction induces a tetrodotoxin-resistant Na+ current in rat cardiomyocytes. J Mol Cell Cardiol 2000;32:1169–1179. [PubMed: 10860761]

15. Amado LC, Gerber BL, Gupta SN, et al. Accurate and objective infarct sizing by contrast-enhanced magnetic resonance imaging in a canine myocardial infarction model. J Am Coll Cardiol 2004;44:2383–2389. [PubMed: 15607402]

16. Ostrzega E, Maddahi J, Honma H, et al. Quantification of left ventricular myocardial mass in humans by nuclear magnetic resonance imaging. Am Heart J 1989;117:444–452. [PubMed: 2916415]

17. International Commission on Radiological Protection. Report of the Task Group on Reference Man: a report prepared by a task group of Committee 2 of the International Commission on Radiological Protection. Pergamon; Oxford, England: 1975.

18. Morady F, DiCarlo L, Winston S, Davis JC, Scheinman MM. A prospective comparison of triple extrastimuli and left ventricular stimulation in studies of ventricular tachycardia induction. Circulation 1984;70:52–57. [PubMed: 6723011]

19. Kleiman RB, Callans DJ, Hook BG, Marchlinski FE. Effectiveness of noninvasive programmed stimulation for initiating ventricular tachyarrhythmias in patients with third-generation implantable cardioverter defibrillators. Pacing Clin Electrophysiol 1994;17:1462–1468. [PubMed: 7991416]

20. Sandstede JJ, Pabst T, Beer M, et al. Assessment of myocardial infarction in humans with 23Na MR imaging: comparison with cine MR imaging and delayed contrast enhancement. Radiology 2001;221:222–228. [PubMed: 11568344]

21. Sandstede J, Pabst T, Beer M, et al. [23]Sodium MRI for infarct imaging of the human heart [in German]. Rofo 2000;172:739–743. [PubMed: 11079085]

22. Pabst T, Sandstede J, Beer M, Kenn W, Neubauer S, Hahn D. Sodium T2* relaxation times in human heart muscle. J Magn Reson Imaging 2002;15:215–218. [PubMed: 11836780]

23. Shimozaki SS, Eckstein MP, Abbey CK. Spatial profiles of local and nonlocal effects upon contrast detection/discrimination from classification images. J Vis 2005;5:45–57. [PubMed: 15831066]

24. Lehr D, Chau R. Changes of the cardiac electrolyte content during development and healing of experimental myocardial infarction. Recent Adv Stud Cardiac Struct Metab 1973;3:721–751. [PubMed: 4806675]

25. Kim RJ, Lima JA, Chen EL, et al. Fast Na-23 magnetic resonance imaging of acute reperfused myocardial infarction: potential to assess myocardial viability. Circulation 1997;95:1877–1885. [PubMed: 9107176]

26. Zipes DP, Wellens HJ. Sudden cardiac death. Circulation 1998;98:2334–2351. [PubMed: 9826323]
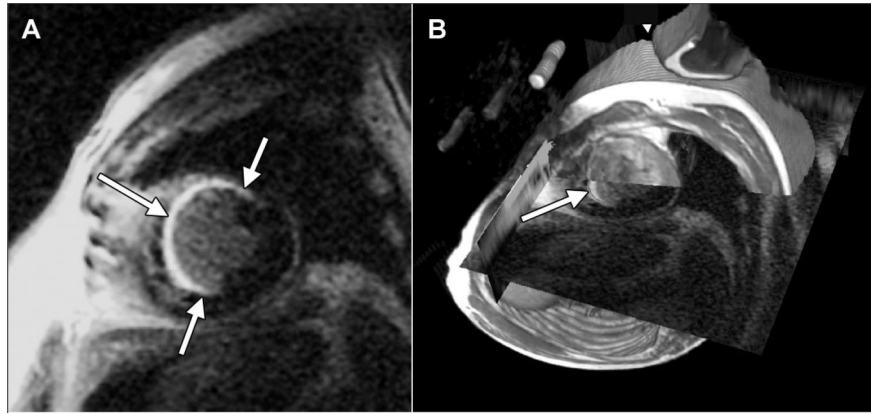
Figure 1.
A, Short-axis delayed contrast-enhanced MR image (5.4/1.3/175, 20° flip angle, 40-cm field of view, 256 × 160 matrix, 8-mm section thickness with 10-mm spacing) in 58-year-old man with extensive MI (arrows). *B*, Image in *A* overlapping ^{1}H fast spin-echo MR image, with cut planes positioned to reveal the intersection of the two data sets on a line through the LV. Landmarks such as the epicardial and endocardial boundaries, aorta, apex, and base are used to guide manual registration of the partially transparent images, which are rendered stereoscopically. Arrow shows position of MI. Fast spin-echo image depicts signals from the three reference phantoms embedded in ^{23}Na coil.
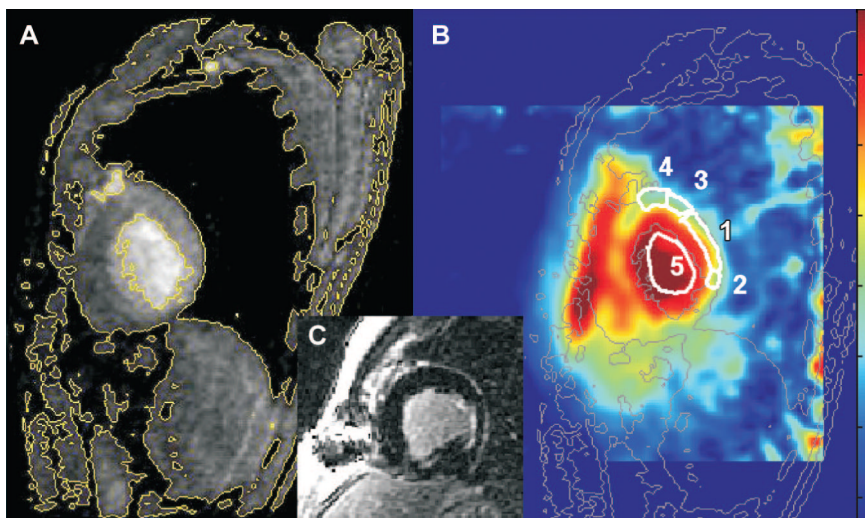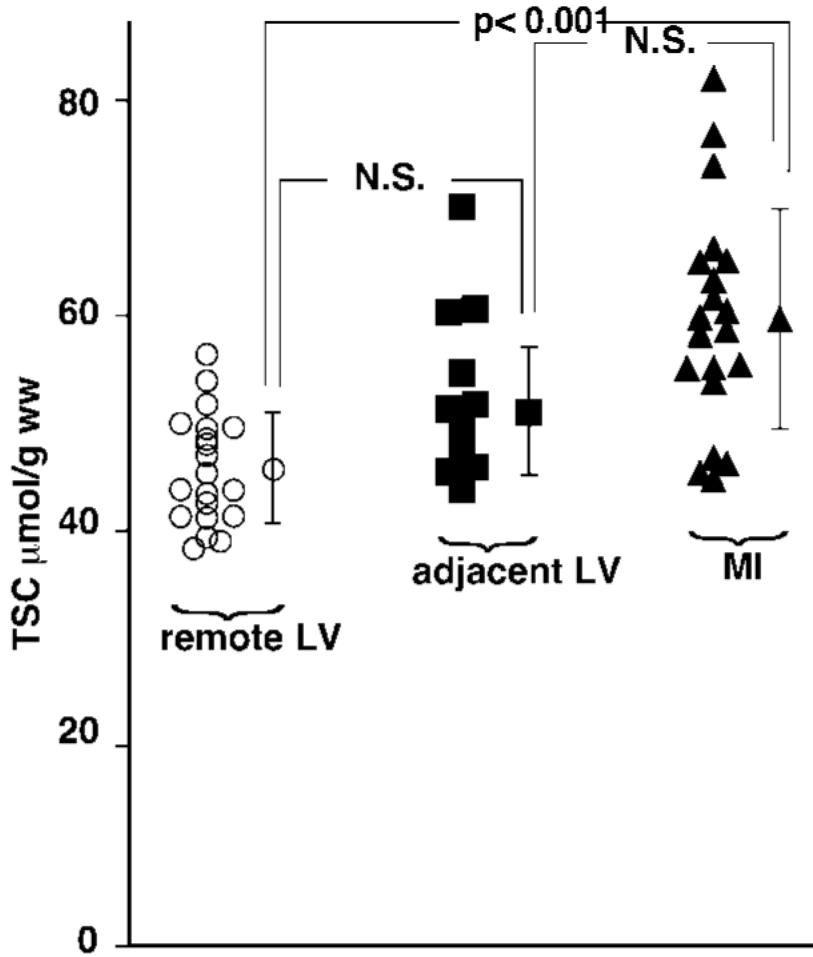
Figure 2.
Sagittal MR images in 53-year-old man with posterior MI show placements of ROIs for quantification of TSC. *A*, Fast gradient-echo ^{1}H image (100/4.2, 90° flip angle, 36-cm field of view, 256 × 192 matrix, 5-mm section thickness) shows signal intensity level contours. The signal intensity level contours outlined in yellow are copied onto corresponding [23]Na image *(B)* (85/0.4, 90° flip angle, 22-cm field of view, three-dimensional twisted spiral acquisition, 6-mm isotropic spatial resolution), where they are outlined in gray. In *B*, ROI *1* is MI used to calculate MI TSC (48 μmol/g wet weight in this patient); ROIs *2* and *3*, adjacent posterior LV wall (TSC, 44 μmol/g wet weight); ROI *4*, noninvolved (remote) LV wall (TSC, 39 μmol/g wet weight); and ROI *5*, LV blood (TSC, 72 μmol/g wet weight). For display purposes, the color scale was designed to be approximately proportional to the sodium concentrations by using a calculated B_1 map of the coil to correct for receiver coil sensitivity. *C*, Short-axis delayed contrast-enhanced image.
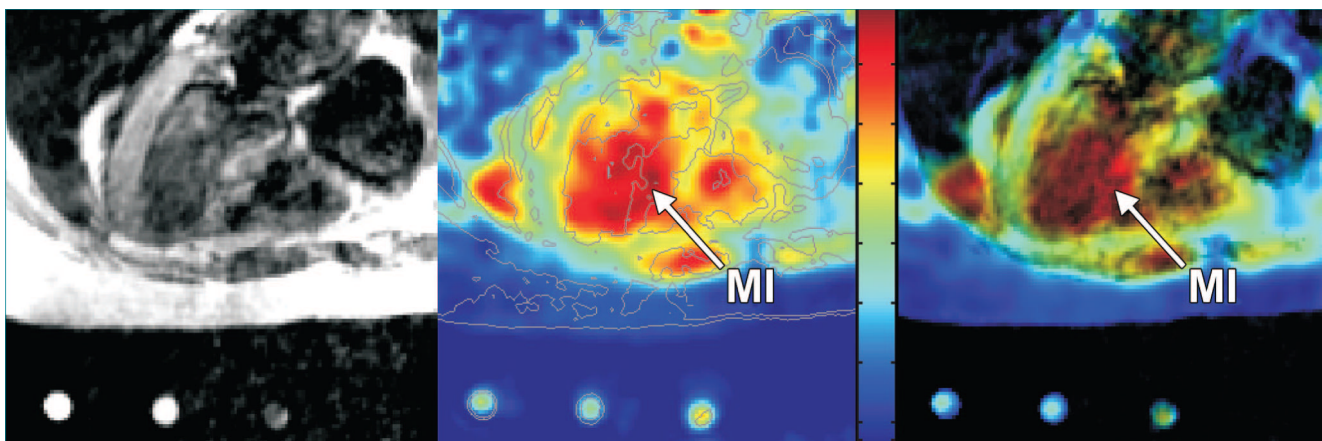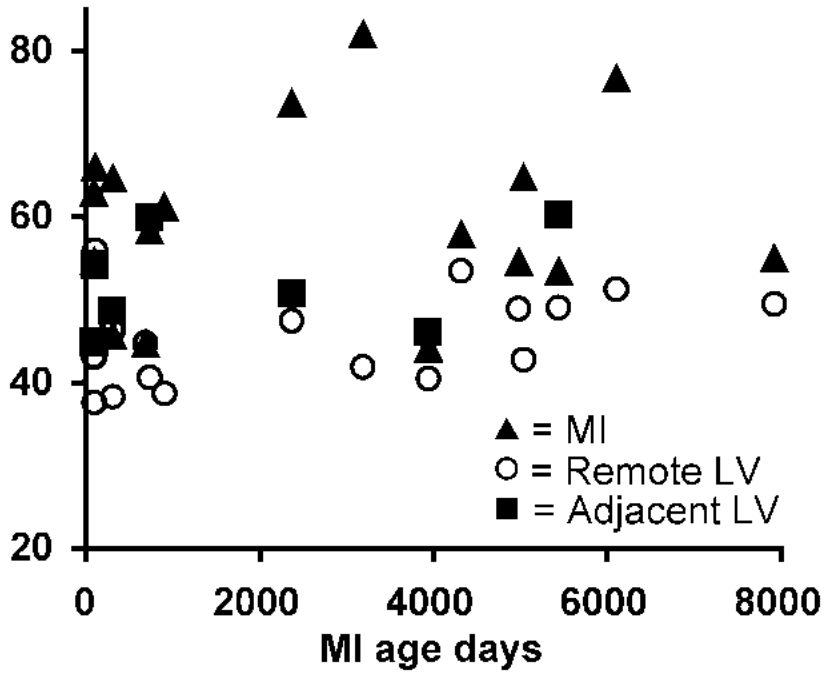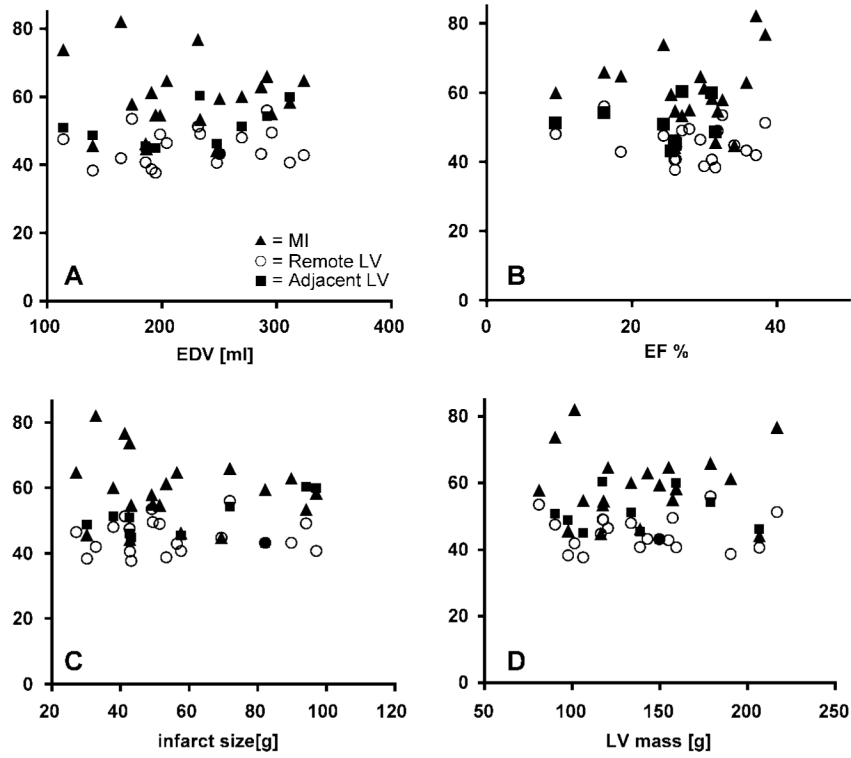
Figure 3.
Axial ^{1}H fast spin-echo MR image (gated to 1 R-R interval, 845/17, echo train length of four, 90° flip angle, 40-cm field of view, 256 × 192 matrix, 7.5-mm section thickness, 2.5-mm intersection gap) merged with corresponding [23]Na twisted projection MR image (85/0.4, 90° flip angle, 22-cm field of view, three-dimensional twisted spiral acquisition, isotropic spatial resolution of 6 mm) in 61-year-old man with remote septal MI (arrows). Left: Fast spin-echo ^{1}H MR image. Middle: Receive coil sensitivity-corrected twisted projection [23]N MR image only, with color scale proportional to TSC and including calculated B_1 correction. Right: Twisted projection [23]Na MR image as a color map overlaid on ^{1}H MR image, with saturation of [23]Na color map modulated by the ^{1}H MR signal intensity such that [23]Na map colors are suppressed in areas where ^{1}H image is dark. Note the increase in sodium signal intensity in the distal part of the septum (arrow), which corresponds to infarcted region determined by delayed contrast-enhanced MR imaging, to nearly the signal intensity of the sodium in the LV blood.
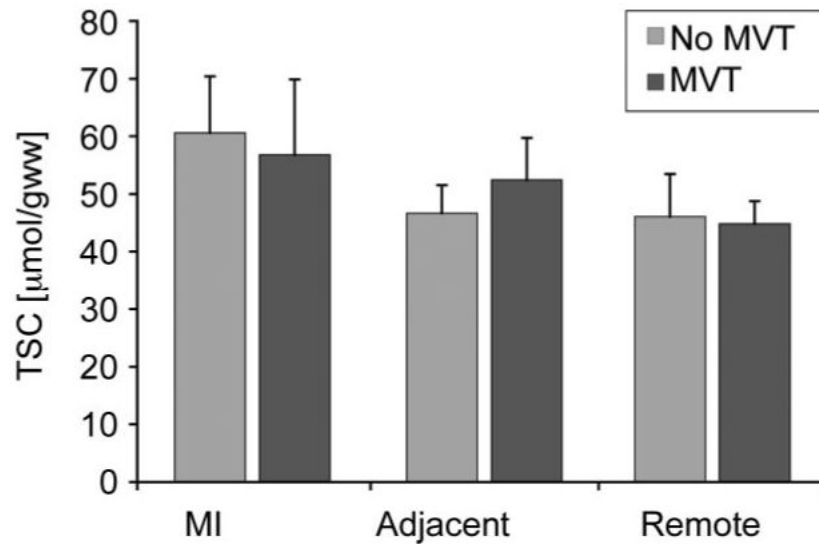
Figure 4.
Graph shows TSC values in MI in 20 patients, in adjacent LV tissue in 11 patients, and in remote LV tissue in 20 patients, with mean values ± 1 standard deviation. MI TSC is significantly increased compared with remote LV TSC, with Bonferroni correction ($\kappa = 3$, $\alpha = .017$). Adjacent LV TSC does not differ significantly from remote region or MI values at similar analysis. *N.S.* = nonsignificant difference.

Figure 5.
Graph shows TSC values in MI, adjacent LV tissue, and remote LV tissue as a function of
infarct age (in days) in the 17 patients in whom infarct age was known. Mean TSC values
measured in infarcted myocardium in each of 20 patients, in remote noninvolved myocardium
in 17 patients, and in adjacent myocardial regions in the eight subjects who had quantifiable
adjacent regions and known infarct age are shown. Some of the older MIs still showed a large
increase in TSC relative to the remote LV, and some younger MIs did not show a substantial
elevation in TSC. Consequently, the correlation between MI TSC and infarct age was poor
(Pearson product moment $r = 0.09$).

Figure 6.
Graphs show TSC values in MI, adjacent LV, and remote LV, which did not correlate with, *A*, end-diastolic volume *(EDV)* (*r* = -0.002, *P* > .05), *B*, ejection fraction *(EF)* (*r* = -0.095, *P* > .05), *C*, absolute infarct size (*r* = -0.16, *P* > .05), or, *D*, LV mass (*r* = 0.005, *P* > .05). Mean TSC values in MI (20 patients), remote noninvolved myocardium (20 patients), and adjacent myocardial regions (11 patients) are shown. Although one might expect the larger infarcts to lead to stress and possibly increased TSC in remote LV tissue or to larger LV mass, or the higher TSC in MI or adjacent tissue to possibly impair cardiac function (as expressed by ejection fraction), no such correlations were apparent from our data.

Figure 7.
Bar graph shows cardiac TSC in MI, adjacent LV tissue, and remote LV regions in nine patients in whom MVT was inducible at electro-physiologic testing and in seven patients in whom MVT was not inducible. For this analysis, adjacent LV tissue was assessed in five patients. Mean TSC in MI was 57 μmol/g wet weight ± 13 for nine patients in inducible group and 61 μmol/g wet weight ± 10 for seven patients in noninducible group (*P* > .05). Mean TSC in adjacent zones assessed in five patients was 54 μmol/g wet weight ± 14 for inducible group and 52 μmol/g wet weight ± 7 for noninducible group (*P* > .05). Mean TSC in remote myocardial tissue was 46 μmol/g wet weight ± 7 for nine patients in inducible group and 45 μmol/g wet weight ± 4 for seven patients in noninducible group (*P* > .05).

Table

TSC Values in Patients and Healthy Control Subjects

Tissue	Patients ($n = 20$)	Control Subjects ($n = 10$)[*]
Remote (µmol/g wet weight)[†]	45 ± 5[‡§]	43 ± 4[‖]
MI (µmol/g wet weight)	59 ± 10[‡‖#]	. . .
Adjacent (µmol/g wet weight) [**]	50 ± 6[§#]	. . .
LV blood (mmol/L)	73 ± 11	88 ± 7
RV blood (mmol/L)	73 ± 12	79 ± 6
Adipose (µmol/g wet weight)	16 ± 5	17 ± 4

Note.—Data are mean values ± standard deviations. RV = right ventricle.

[*] Reference 12.

[†] Noninvolved LV myocardium excluding the septum.

[‡] $P < .001$ (paired t test) for comparison between MI and noninvolved (remote) LV values in patients. Difference remained significant after Bonferroni correction ($\alpha = .017$, $\kappa = 3$).

[§] $P < .04$ (paired t test) for comparison between adjacent LV and remote LV values. Difference was not significant after Bonferroni correction ($\alpha = .017$, $\kappa = 3$).

[‖] $P < .001$ (two-tailed t test) for comparison between TSC in MI and TSC in corresponding remote LV in healthy control subjects.

[#] $P < .06$ (paired t test) for comparison between adjacent LV and MI values in 11 patients. Difference was not significant after Bonferroni correction ($\alpha = .017$, $\kappa = 3$).

[**] Adjacent myocardial regions bordering the MIs were identified with delayed contrast-enhanced MR imaging in 11 of the 20 patients.